Towards the On-Chip Realization of Polarization Encoded QuBits

Duncan L. MacFarlane[a], Adam Helmy[a], Hiva Shahoei[a], Tim LaFave Jr.[a], Mitchell A. Thornton[a], Evan Stewart[b] and Wil Oxford[b]
[a]The Darwin Deason Institute for Cybersecurity, Southern Methodist University, Dallas, Texas;
[b]Anametric, Inc. Austin, Texas

ABSTRACT

While photonic quantum circuits may be implemented using polarization-encoded qubits, their photonic integrated circuit (PIC) realization has been limited by on-chip impairments such as mode dispersion and polarization state stability that do not hinder bulk-optic, table-top setups. In this paper, we will present an interpretation of on-chip polarization and provide the beginning of a portfolio of components that may be used for polarization-encoded qubits. Central to our work is the use of waveguides of square cross-section, which symmetrically support orthogonal TE and TM modes with perpendicular electric fields. Preliminary designs for components to manipulate these modes are presented, along with measurements relevant to polarization in PICs. The research has relevance, as well, to sensing and security.

Keywords: Quantum Photonic Integrated Circuits, square waveguides

1. INTRODUCTION

While many photonic quantum circuits may be implemented using polarization-encoded qubits, their photonic integrated circuit (PIC) realization has been limited by on-chip impairments such as mode dispersion and polarization state stability that do not hinder bulk-optic, table-top setups. In addition, there are, now, routinely successful transmissions of polarization-entangled qubits through fiber optic channels of useful distances. For size, weight, and power considerations, it is desirable to support both quantum informatic calculation and quantum communication applications with quantum PICs. However, many PIC components are optimized for communication and microwave photonic applications that benefit from single-mode operation. Given this constraint, a successful route to date for developing quantum photonic integrated circuitry has been spatial, Fock state, and squeezed-state encoding. Some algorithms unfortunately do not match well with this approach, perhaps because certain components do not readily exist in an integrated photonic realization. In this paper, we present an interpretation of on-chip polarization and provide the beginning of a portfolio of components that may be used for polarization-encoded qubits. Central to our work is the use of waveguides of square cross-section that symmetrically support orthogonal TE and TM modes with perpendicular electric fields. Preliminary designs for components to manipulate these modes are presented based on simulations performed primarily in Lumerical's MODE: Waveguide Simulator[Lumerical Inc.] relevant to polarization in PICs. The research has relevance, as well, to sensing and security.

Silicon photonics has a long and sustained development history [1-4], and for that reason we begin this paper with this material choice. Further, single photon pair production in Si ring resonators is readily available, and C-band operation supports current classical and quantum fiber optic communication work [3-5].

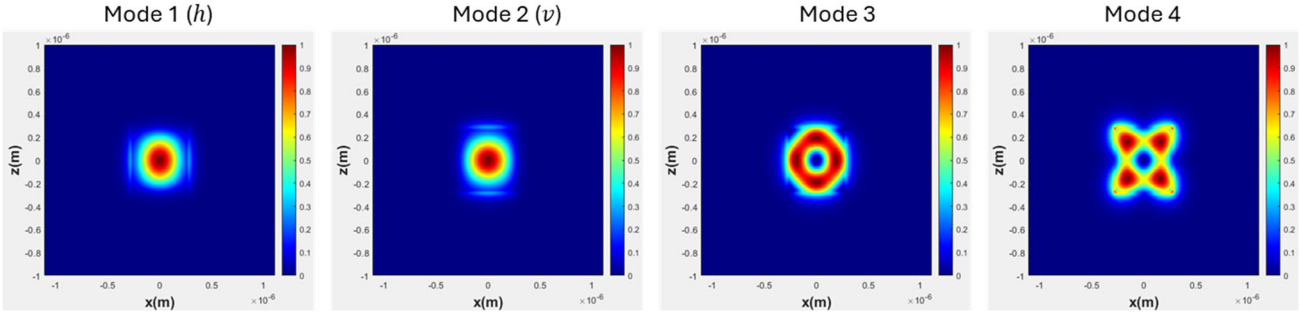

Figure 1. Total electric field amplitudes for the first 4 modes supported by a 550 nm × 550 nm square Si/SiO_2 waveguide.

Among the few investigations of square waveguides has been interest in iris polarizers for square metal waveguides feeding square aperture antennas in the Ku-band [6-8] and more recently in the Ka-band [9]. Twisted square metal waveguides have also been studied [10]. Square silicon waveguides have been used in two dimensional arrays to image 1530 nm - 1570 nm light [11]. One reason for the shortage of research into waveguides of square symmetry is the preference of many circuit and system designers for one dominant mode. Another reason may be that many devices, such as semiconductor lasers, are necessarily (approximately) rectangular. We note as well, the prevalence of singular mode rectangular waveguide examples taught in electromagnetic textbooks and courses [12-14], and to be fair, square symmetry is covered as a special case of rectangular geometry [15]. Our research group has seen success in deploying square cross-section TOPAS waveguides for polarization-multiplexed THz communication links [16-19]. Square cross-section vortex fibers for THz orbital angular mode multiplexing have also been demonstrated [20]. Other recent work in square symmetry integrated photonics include a design of an array waveguide [21], a design for very low index geometry invariant waveguides [22] and designs for polarization rotators [23,24].

2. RESULTS

In Figure 1 is shown the total electric field distribution of the first four modes supported by a 550 nm × 550 nm square cross-section waveguide comprising a Si core and SiO_2 cladding for wavelength $\lambda = 1550$ nm.. In this paper, we will focus on the first two modes, h and v. Though the underlying components of the electric field differ between pairs, their total fields are nearly identical, and they share the same effective index of refraction. In the long run, silicon nitride (Si_3N_4)will likely provide a versatile material platform for visible to mid-IR operation. However, in this paper we will focus on square Si waveguides. We note that the 550 nm height presented here is a necessary departure from many Si photonic foundries.

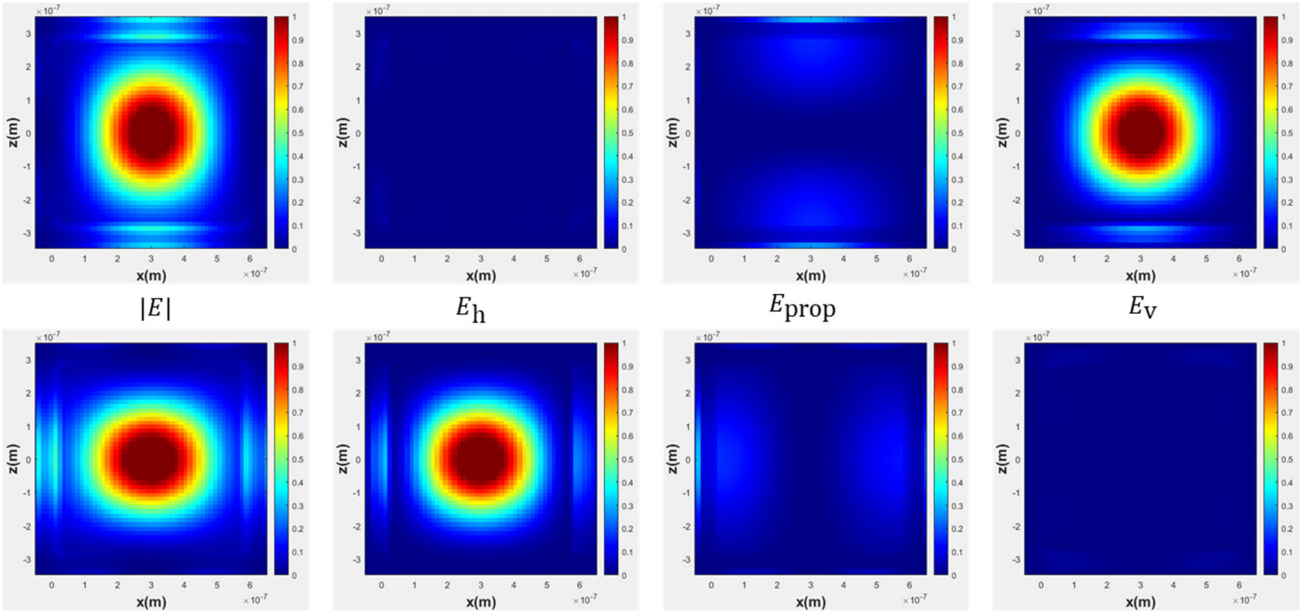

Figure 2. Electric field components for modes 1 (vertical, shown in the top row) and 2 (horizontal, shown in the bottom row) of a 550 nm × 500 nm square Si/SiO_2 waveguide. In addition to the mode magnitude, the components in the horizontal, propagation and vertical directions are shown.

In Figure 2 are shown the electric field components for modes 1 and 2 shown in Fig. 1. To avoid confusion, these respective mode components are labeled relative to the invariants of the photonic integrated circuit (PIC) geometry envisioned herein, namely horizontal, h, vertical, v, and for the direction of propagation, $prop$. Given the dominant electric field components of modes 1 and 2, these modes are referred to as vertical, v, and horizontal, h, respectively. As verified numerically, these modes are orthogonal. Further, linear combinations of the h and v modes also propagate at the same velocity as the individual h and v modes.

Degeneracy of h and v modes results from the square symmetry of the waveguide and gives rise to utility, particularly in the context of polarization encoding of single and few-photon informatic applications. Judicious breaking of this symmetry

enables further utility in the form of polarization-sensitive components. For example, curving, narrowing or widening the waveguide in one dimension, or placing additional waveguides parallel to the first affect the two modes differently.

Not all broken symmetries distinguish significantly between h and v mode components. Figure 3 shows the propagation of the h and v modes through a typical Y-coupler, redesigned for waveguides with square cross-sections. In quantum informatics, the ability to equally split single photons of arbitrary polarization is useful. The Bell inequality test for quantized behavior, for example, is widely deployed. Homodyne detection for enhanced signal-to-noise ratio (SNR) is another application. In the Y-coupler shown, the v-mode splitting is perfectly symmetric with -3.30 dB in each branch. The h-mode is mildly asymmetric with -3.35 dB in the top branch and 3.31 dB in the bottom branch.

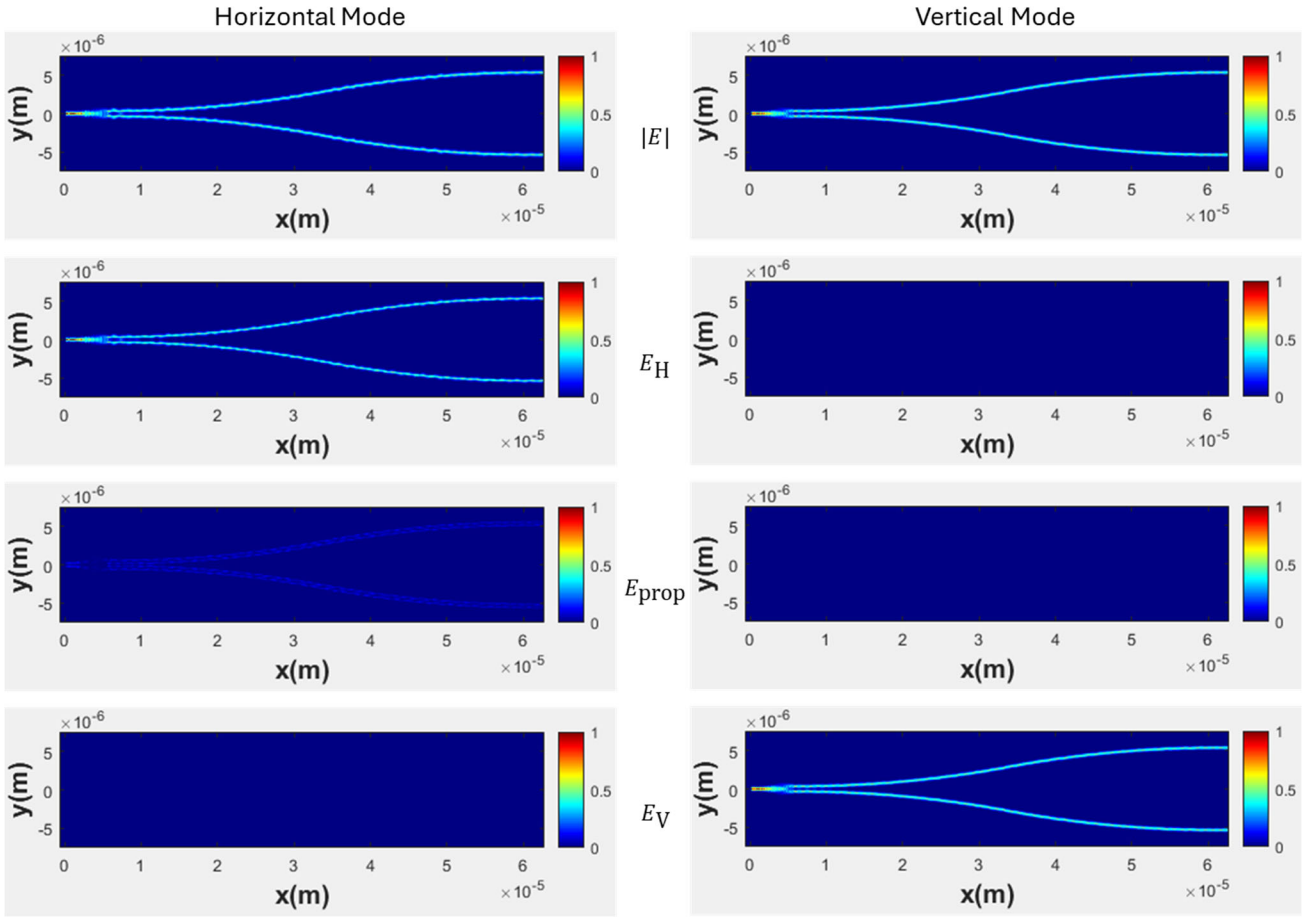

Figure 3. Electric field components for the horizontal and vertical modes propagating in a conventional Y-coupler.

Conversely, a mode splitter – a polarizing beamsplitter – may be realized using two closely spaced parallel waveguides, because the v-mode exhibits stronger coupling than the h-mode. Figure 4 shows a top view of the coupling behavior of two parallel 550 nm × 550 nm square Si/SiO_2 waveguides separated by 100 nm. The v mode couples quickly with a coupling period of ~13.5 μm, compared with a coupling period of ~37.5 μm for the h mode. Interestingly, good crosstalk-free v-mode coupling occurs at three periods. At this point, 97% of the v mode and 1% of the h-mode are coupled with a loss of 2%.

By adjusting the spacing and the total interaction length, equal splitting of both of the two modes simultaneously may be achieved. One example of suitable dimensions for this component is a 75 nm gap between the two parallel waveguides with a ~38 μm coupling length. The modes for this splitter are less distorted than the Y-coupler shown in Fig. 3.

Evanescent coupling for more complicated geometries is made more difficult by the different interaction lengths. It is challenging, for example, to find a robust design for a ring resonator that supports both h mode and v mode operation equally. One challenge is to balance the coupling that is different for the different modes. However, with the mode splitter

shown in Fig. 4, single mode rings may be utilized. Further, two separate single mode ring resonators may be implemented – one on each of the two output waveguides of the mode-splitter in Fig. 4.

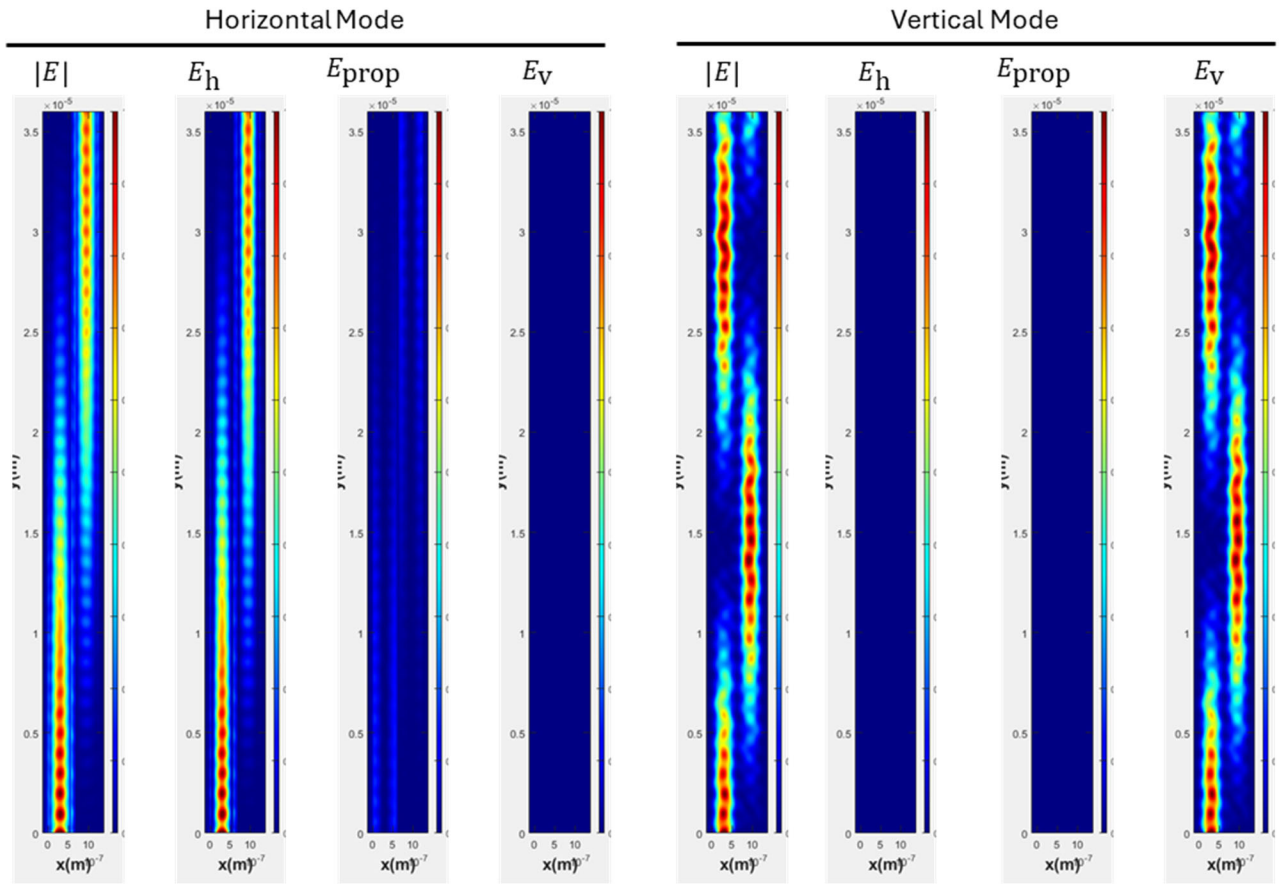

Figure 4. Electric field coupling between two parallel 550 nm × 550 nm square cross section waveguides separated by 100 nm. The waveguides have Si cores buried in SiO_2 that serves as the cladding.

Our final example of a polarization component realized in a square waveguide geometry is a $\lambda/2$ waveplate based on a taper. Since the effective index of a square waveguide is a function of the dimensions of the waveguide, tapering in one direction provides a different propagation speed for the h-mode relative to the v-mode. Using this break in symmetry introduces a π-phase shift between the h mode and the v mode. In Fig. 5 is shown the input and output mode character of a V-shaped taper. For Fig. 5, the horizontal width of the waveguide first tapers down to 400 nm within a length of 7.5 μm and then increases back up to 550 nm within a second 7.5 μm length of expanding taper. The input mode in Fig. 5 is a 50:50 superposition of h-mode and v-mode components, The output is also an equal mixture of h-mode and v-mode with the phase difference rotated, however, by 90°. The loss in this waveplate is ~1%.

3. CONCLUSIONS

In this paper, we have reported the simulated behavior of optical modes within a silicon dielectric waveguide of 550 nm × 550 nm square geometry at $\lambda = 1550$ nm and have presented designs for several useful components. Discussed were 1×2 couplers including one that evenly splits modes and one that separates the two orthogonal, degenerate, lower-order modes. In a Si/SiO_2 directional coupler, we demonstrated that a v mode couples more quickly (~13.5 μm) than the corresponding h mode (~37.5 μm) across a 100 nm gap. At three periods in length, only 2% loss occurs with 97% of the v mode and 1% of the h-mode coupled. In addition, the use of tapers was introduced to realize waveplates.

Photonics, and quantum photonics will benefit from a library of polarization components, and we have presented a few. Additions to this list are numerous, from the practical (symmetric edge couplers are needed to move polarization

information onto and off of PICs) to the fundamental (readily fabricated waveplates and tunable waveplates will allow more polarization-based operations). For coherence, we have presented work in silicon at 1550. Silicon Nitride will grow in importance at 1550 and will open the door to shorter wavelengths.

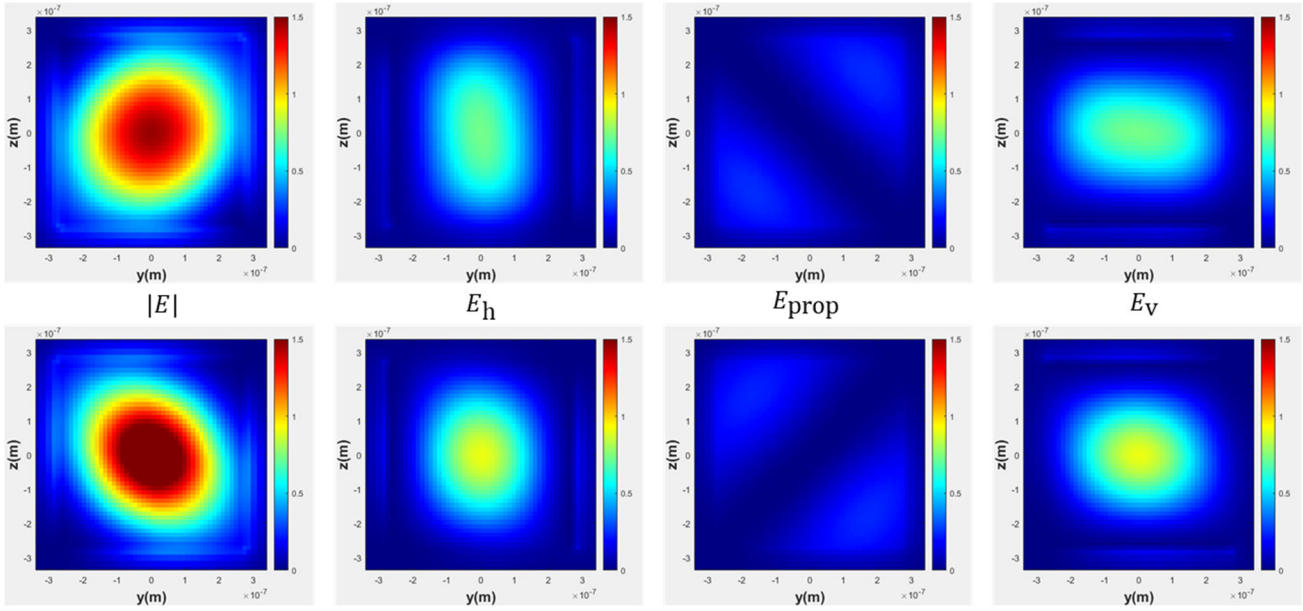

Figure 5. Input and output electric field components phases are rotated by 90° using a V-shaped taper. This geometry provides for a waveplate.

REFERENCES

[1] Soref, R. A. and Lorenzo, J. P., "All-Silicon active and passive guided-wave components for lambda 1.3 and 1.6 μm," IEEE J. Quantum Electron. QE-22(6), 873–880 (1986). doi: 10.1109/JQE.1986.1073057

[2] Paniccia, M., Morse, M., Salib, M. Integrated Photonics. In: Silicon Photonics. Topics in Applied Physics, vol 94. Springer, Berlin, Heidelberg. (2004). doi: 10.1007/978-3-540-39913-1_2

[3] Won, R. Integrating silicon photonics. Nature Photon 4, 498–499 (2010). doi: 10.1038/nphoton.2010.189

[4] Yikai Su; Yong Zhang, Chapter 1: History and Current Status, in Passive Silicon Photonic Devices: Design, Fabrication, and Testing, AIPP Books, 2022. doi: 10.1063/9780735424319_001

[5] Assia Barkai, Yoel Chetrit, Oded Cohen, Rami Cohen, Nomi Elek, Eyal Ginsburg, Stas Litski, Albert Michaeli, Omri Raday, Doron Rubin, Gadi Sarid, Nahum Izhaky, Mike Morse, Olufemi Dosunmu, Ansheng Liu, Ling Liao, Haisheng Rong, Ying-hao Kuo, Shengbo Xu, Drew Alduino, Jeffrey Tseng, Hai-Feng Liu, and Mario Paniccia, "Integrated silicon photonics for optical networks [Invited]," J. Opt. Netw. 6, 25-47 (2007). doi: 10.1364/JON.6.000025

[6] U. Tucholke, F. Arndt and T. Wriedt, "Field Theory Design of Square Waveguide Iris Polarizers," in IEEE Transactions on Microwave Theory and Techniques, vol. 34, no. 1, pp. 156-160, Jan 1986, doi: 10.1109/TMTT.1986.1133293.

[7] M. H. Chen, G. N. Tsandoulas and F. G. Willwerth, "Modal Characteristics of Quadruple-Ridged Circular and Square Waveguides (Short Papers)," in IEEE Transactions on Microwave Theory and Techniques, vol. 22, no. 8, pp. 801-804, Aug. 1974, doi: 10.1109/TMTT.1974.1128341.

[8] W. Sun and C. A. Balanis, "Analysis and design of quadruple-ridged waveguides," in IEEE Transactions on Microwave Theory and Techniques, vol. 42, no. 12, pp. 2201-2207, Dec. 1994, doi: 10.1109/22.339743.

[9] Piltyay, S. (2021). Square Waveguide Polarizer with Diagonally Located Irises for Ka-Band Antenna Systems. Advanced Electromagnetics, 10(3), 31–38. https://doi.org/10.7716/aem.v10i3.1780

[10] L. Lewin and T. Ruehle, "Propagation in Twisted Square Waveguide," in IEEE Transactions on Microwave Theory and Techniques, vol. 28, no. 1, pp. 44-48, Jan. 1980, doi: 10.1109/TMTT.1980.1130004

[11] Hui Chen and D. T. K. Tong, "Two-dimensional symmetric multimode interferences in silicon square waveguides," in IEEE Photonics Technology Letters, vol. 17, no. 4, pp. 801-803, April 2005, doi: 10.1109/LPT.2004.843257.
[12] John C. Slater and Nathaniel Frank, Electromagnetism 1947, Dover Publications, Inc. New York.
[13] John D, Jackson, Classical Electrodynamics 2nd Edition, 1975, John Wiley and Sons. New York.
[14] David M. Pozar, Microwave Engineering, 2nd Edition, 1998, John Wiley and Sons. New York.
[15] Frédéric Grillot, Laurent Vivien, Suzanne Laval, and Eric Cassan, "Propagation Loss in Single-Mode Ultrasmall Square Silicon-on-Insulator Optical Waveguides," J. Lightwave Technol. 24, 891- (2006)
[16] N. Aflakian, N. Yang, T. LaFave, R. M. Henderson, K. K. O, and D. L. MacFarlane, "Square dielectric THz waveguides," Opt. Express 24, 14951-14959 (2016). doi: 10.1364/OE.24.014951
[17] N. Aflakian, M. Gomez, C. Miller, R. Henderson, D. MacFarlane and K. K. O, "Functional Performance of a Millimeter Wave Square Holey Dielectric Waveguide," 2019 IEEE Radio and Wireless Symposium (RWS), Orlando, FL, USA, 2019, pp. 1-4, doi: 10.1109/RWS.2019.8714541.
[18] S. Wane and N. Aflakian, "Photonics Chip-to-Chip Communication for Emerging Technologies: Requirements for Unified RF, Millimeter-Waves and Optical Sensing," 2019 IEEE Texas Symposium on Wireless and Microwave Circuits and Systems (WMCS), Waco, TX, USA, 2019, pp. 1-5, doi: 10.1109/WMCaS.2019.8732547.
[19] Mukul Mishra, Neha Mahendarkar, Het Pranav Trivedi, Rashaunda Henderson, Ibunkunoluwa Momson, Michael Gomez, Nafiseh Aflakian, Zhe Chen, K. O Kenneth. Duncan MacFarlane, "Waveguide Excitation Using On-Chip Antenna for Wireline Data Links," 2019 IEEE International Conference on Microwaves, Antennas, Communications and Electronic Systems (COMCAS), Tel-Aviv, Israel, 2019, pp. 1-4, doi: 10.1109/COMCAS44984.2019.8958239.
[20] Nafiseh Aflakian, Tim P. LaFave, K. O. Kenneth, Solyman Ashrafi, and Duncan L. MacFarlane, "Design, fabrication, and demonstration of a dielectric vortex waveguide in the sub-terahertz region," Appl. Opt. 56, 7123-7129 (2017). doi: 10.1364/AO.56.007123
[21] Gatkine, Pradip, et al. "Potential of commercial SiN MPW platforms for developing mid/high-resolution integrated photonic spectrographs for astronomy." Applied Optics 60.19 (2021): D15-D32.
[22] Wang, Danqing, Dong, Kaichen, Li, Jingang, Grigoropoulos, Costas, Yao, Jie, Hong, Jin and Wu, Junqiao. "Low-loss, geometry-invariant optical waveguides with near-zero-index materials" Nanophotonics, vol. 11, no. 21, 2022, pp. 4747-4753. https://doi.org/10.1515/nanoph-2022-0445
[23] Hsiao F-L, Ni C-Y, Tsai Y-P, Chiang T-W, Yang Y-T, Fan C-J, Chang H-M, Chen C-C, Lee H-F, Lin B-S, et al. Design of Waveguide Polarization Convertor Based on Asymmetric 1D Photonic Crystals. Nanomaterials. 2022; 12(14):2454. https://doi.org/10.3390/nano12142454
[24] Liu L-Y, Huang H-C, Chen C-W, Hsiao F-L, Cheng Y-C, Chen C-C. Design of Reflective Polarization Rotator in Silicon Waveguide. Nanomaterials. 2022; 12(20):3694. https://doi.org/10.3390/nano12203694